Imaging of carrier dynamics in semiconductor heterostructures by surface acoustic waves

M. Streibl[a,*], A. Wixforth[a], J.P. Kotthaus[a], C. Kadow[b], A.C. Gossard[b]

[a] *Sektion Physik and CeNS der LMU München, Geschwister-Scholl-Platz 1, D-80539 München, Germany*
[b] *Materials Department and QUEST, University of California, Santa Barbara, CA 93106, USA*

Abstract

Surface acoustic waves (SAW) are an ideal tool for the noninvasive detection of conductivity and carrier distributions in otherwise unstructured semiconductor systems. Here we demonstrate a technique that allows for spatially resolved experiments with a resolution of a few acoustic wavelengths. Extremely narrow acoustic paths, excited by tapered interdigital transducers, are employed to probe conductivity profiles. The method is used to resolve the spatial form of a photogenerated electron–hole plasma and allows for the direct observation of room-temperature drag and transport of electrons and holes in the coherent phonon wind of an intense SAW beam. By the application of a tomographic technique we are able to reconstruct 2D charge distributions.

PACS: 43.20.H; 43.35.S; 72.20; 43.38.R; 63.20.L; 43.38

Keywords: Surface acoustic wave; Semiconductor; Imaging; Phonon wind

On piezoelectric substrates like most of the III/V materials are, surface acoustic waves are accompanied by strong piezoelectric fields. On GaAs heterostructures vertical and lateral fields on the order of 10^4 to 10^5 V/cm are achievable. Just as these fields modulate the electrical and optical properties of a quantum well system, free carriers in the wells influence the waves propagation by dynamic screening. The interaction of carriers and the waves fields leads to a decrease of the wave velocity. In general for a conducting sheet near the surface with conductivity σ the change in velocity is given by [1]

$$\frac{v}{v} = \frac{K_{\text{eff}}^2}{2} \frac{1}{1 + (\sigma/\sigma_{\text{m}})^2}, \tag{1}$$

where K_{eff}^2 is the electromechanical coupling constant (6.4×10^{-4} for GaAs) and σ_{m} gives the crititical conductivity where the energy transfer from the SAW to the electron system is maximum, i.e. the screening currents are dissipative. The energy loss by screening currents leads to a damping of the acoustic waves which is characterized by the damping constant

$$\Gamma = \frac{K_{\text{eff}}}{2} k_{\text{SAW}} \frac{/\sigma_{\text{m}}}{1 + (\sigma/\sigma_{\text{m}})^2}. \tag{2}$$

* Corresponding author. Tel.: +49-2180-3721; fax: +49-2180-3182.
E-mail address: martin.streibl@physik.uni-muenchen.de (M. Streibl)

The measurement of the SAW intensity and the propagation velocity, respectively, provides a simple and extremely sensitive method for the determination of the dynamic conductivity $\sigma(\omega, k)$ of carriers in a semiconductor structure. It has been extensively used for the investigation of properties of a two-dimensional electron system in the quantum Hall regime [2] and in the fractional quantum Hall regime [3] where it played an important role in the experimental verification of the composite fermion picture.

In this paper we present a modification of the SAW scanning of charge distributions by introducing an additional spatial resolution of a few acoustic wavelengths, i.e. usually a few micrometers. Its high sensitivity even at room temperature enables us to study the shape and dynamics of photogenerated carrier profiles in detail.

Surface acoustic waves are usually generated by interdigitated transducers (IDT). When a high-frequency voltage signal is applied to the interdigitated gate structure on the semiconductors surface the piezoelectric crystal is periodically deformed. The propagating deformations superpose constructively if the resonance condition $df_0 = v_{\mathrm{SAW}}$ is met, where f_0 is the resonance frequency, d is the periodicity of the IDT and v_{SAW} is the speed of sound. On the weakly piezoelectric GaAs many transducer periods are necessary to achieve high SAW amplitudes. However an increased number of periods simultaneously reduces the bandwidth of the IDTs resonance which is expressed by

$$P_{\mathrm{SAW}} \propto N^2 \frac{\sin^2 f'}{f'^2}, \tag{3}$$

where P_{SAW} is the acoustic power, $f' = N\pi(f - f_0)/f_0$ and N is the number of transducer periods. Typical values in our experiments are $N = 100$ and $f_0 = 1$ GHz so the bandpass Δf is approximately $f_0 = f_0/N = 10$ MHz. In fact, because of internal reflections of the SAW within the transducer the effective bandpass is reduced even more to only a few MHz. Our experiments are based on this high selectivity in frequency space. When the periodicity of the transducer is varied linearly on its length as shown in Fig. 1 also the resonance condition is spatially modulated. This leads to a correlation between the frequency f of the applied voltage signal and the position in the transducer where resonance occurs and the SAW is launched.

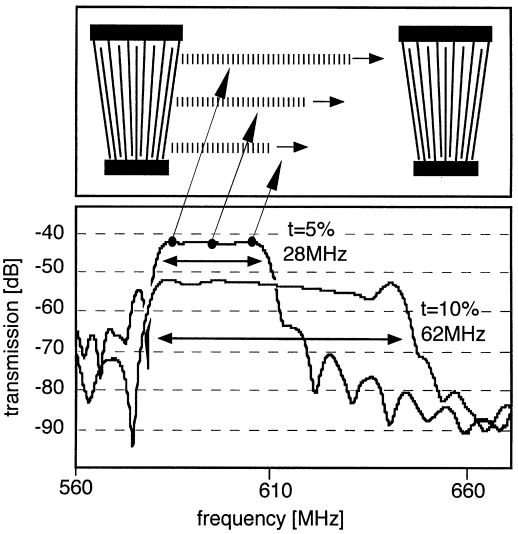

Fig. 1. SAW transmission of tapered IDTs with variation of the transducer periodicity of 5% and 10%. The usually sharp transmission is broadend to a bandpass of 28 and 64 MHz, respectively. The upper half indicates the correspondence between a point in frequency space and the origin of the SAW beam in real space.

The so-called tapered IDTs enable us to adjust the vertical position of the SAW beam by varying f. Moreover the fan shape of the transducer results in a band-spread of the sharp transmission corresponding to the relative variation $t = \Delta d/d$ of the IDT period. Fig. 1 shows the resulting bandpasses for $N = 100$ and tapering factors of $t = 5\%$ and 10%, respectively. The upper panel indicates the correspondence between frequency space and real space. Each point of the bandpass corresponds to a single point of resonance in the IDT, where the narrow SAW beam is launched. The width of the beam is approximately $w = L/Nt$ where L is the IDT aperture. For our 560 MHz IDT with $t =$ 10% and aperture $L = 400$ μm we expect $w = 40$ μm. In fact most of the SAWs energy is found within a much smaller core region. In X-ray topography experiments at the ESRF in Grenoble as described by Sauer et al. [4] the generation of such an adjustable narrow SAW beam could directly be confirmed. Like a radar beam the narrow SAW path can be used to scan the charge distribution between the two IDTs. This is economically done by a network analyzer which auto-

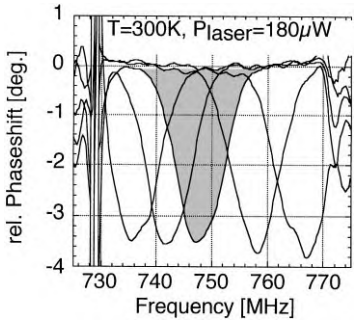

Fig. 2. Phase shift signal induced by a photogenerated electron–hole plasma within the SAW path. The different traces correspond to different positions of the laser spot on the sample.

matically does the frequency sweep and records phase and amplitude of the transmitted SAW.

The simplest object to test the imaging technique is an electron–hole plasma (EHP) generated by a μm laser spot. In our experiments we used a Ti-sapphire laser to excite carriers selectively only in the quantum wells of an InGaAs heterostructure midway between the IDTs. Typical laser intensities were 100 μW. The IDTs were fabricated by e-beam lithography and had an electrical period of $d = 4$ μm and a center frequency of 750 MHz corresponding to a SAW velocity $v_{\mathrm{SAW}} = 2865$ m/s for GaAs.

We measured the phase shift of the transmitted acoustic wave as a function of the exciting frequency as shown in Fig. 2. Different traces for different laser spot positions were taken. A maximum phase shift is observed at the frequency where the scanning SAW beam hits the core of the EHP. To evaluate the data we calculate the expected shape of the phase shift signal. For simplicity, a Gaussian conductivity profile $(x, y) = \sigma_0\sigma_{\mathrm{m}}\exp(-(x^2 + y^2)/r^2)$ for the EHP is assumed. The constant σ_0 here gives the peak conductivity in units of the critical conductivity σ_{m}. From the reduction of SAW velocity given by Eq. (1) the phase shift is calculated and integrated along each acoustic path crossing the Gaussian distribution. Numerical fitting of the theory trace to the data nicely reproduces the shape of the peaks and allows for the extraction of the width r and the maximum conductivity σ of the EHP. For the phase shift measurements in Fig. 2 we get a width of $r = 66$ μm and $\sigma = 1.46\sigma_{\mathrm{m}}$. What width would be expected? The diffusive expansion of the EHP is described by $r^2(t) = r_0^2 + 4Dt$ where D is the diffusion constant and r_0 the initial radius. From electron–hole lifetime measurements on the same quantum well structure we know that the average lifetime is $\tau = 20$ ns at room temperature. So we can estimate the diffusion constant to be $D \approx 540$ cm^2/s.

A series of publications demonstrated that the dynamics of a EHP is at least at low tempertures governed by a phonon wind mechanism [5,6]. The thermalization of photoexcited carriers in the laser spot leads to a so-called phonon hot spot which emits ballistic phonons. Electrons and holes follow the phonon wind with the speed of sound so that the width of the charge distribution is determined by τv_{s} where v_{s} is the sound velocity.

Surface acoustic waves provide a coherent phonon wind and so demonstrate the interaction of carriers and phonons in its purest form. At sufficient amplitudes they can be used to capture and transport carriers in their traveling piezoelectric potential superlattice [7]. On hybrid systems, i.e. the combination of strong piezoelectic materials like $LiNbO_3$ with the excellent electronic properties of AlGaAs heterostructures the rending of a two-dimensional electron system into propagating stripes of carriers could be achieved with high efficiency by Rotter et al. [8]. The SAW imaging technique presented here can be applied for the direct observation of carrier localization in the SAWs propagating potential pattern. For this experiment a sample with an additional SAW path, orthogonal to the probing SAW path was fabricated. This second SAW beam was designed to provide high SAW amplitudes and in fact converted more than 10% of the electrical signal into acoustic power. Fig. 3 shows a typical measurement. The inset schematically depicts the two SAW paths. The vertical SAW beam provides the phonon wind to pump carriers away from the laser spot. The horizontal probing SAW beam generated by tapered IDTs measures the conductivity profile in and around the laser spot. Fig. 3 shows two scans of the EHP. The solid line was taken with and the broken line without orthogonal phonon wind, which yields two effects: First the reduction of the EHP density in the laser spot and a shift of the plasma core along with the phonon wind; Secondly a charge transport tail which indicates the effective trapping of carriers in the coherent phonon wind of the pump SAW beam.

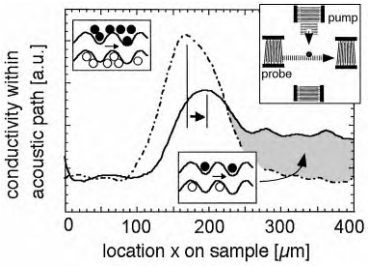

Fig. 3. Phase shift induced by a laserspot in the SAW path. The inset shows the experimental setup. The broken line is taken without and the solid line with an additional vertical pump SAW. Carrier drag of the EHP core and carrier trapping and transport in the coherent phonon wind of the intense pump beam is observed.

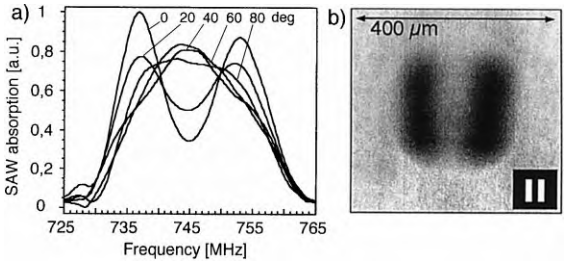

Fig. 4. (a) Scans of the charge distribution induced by the optical projection of a double slit aperture at various angles; (b) Reconstruction of the 2D charge distribution by standard tomography backprojection techniques.

The captured electrons and holes are transported over macroscopic distances, on the order of millimeters as shown in the experiment.

In the core region of the EHP the piezoelectric fields of the pump SAW are dynamically screened. The residual fields are not sufficient for charge separation and trapping. However momentum is still transfered from the SAW to the EHP which results in the observed peak shift. In the transport regime electrons and holes find their respective potential minimum half a wavelength apart from each other, resulting in an effective suppression of their radiative decay. Compared to the experiments by Rocke et al. [7] the sensitivity of our method is high even at room temperature and allows for a direct comparison of the number of injected and transported carriers. Rocke et al. found a transport efficiency of about 20% at $T = 4.2$ K. From the ratio of the conductivity within the EHP core and the transport tail we can extract an even higher transport efficiency of up to 50% at room temperature for our InGaAs quantum well system. When repeated for various SAW amplitudes and laser intensities the presented experiments outline the dependence of the transport efficiency on SAW amplitude and carrier density and provide guidelines for the application of charge conveyance in optoelectronic devices. A detailed discussion however is beyond the scope of this paper and will be given elsewhere [9].

Up to now we only concentrated on 1D scans of charge distributions. When complex 2D carrier profiles should be scanned as might be interesting for imaging applications we can borrow basic principles of computer tomography to reconstruct 2D pictures from a series of 1D scans. In our case this would mean to roentgenize a 2D charge profile by probing SAW beams from various angles. To keep the experiment simple, we went the other way round and rotated the 2D charge profile on a fixed SAW path. Experimentally this is achieved by exchanging the laser of our previous experiments by a white light source which projects a slide onto the sample. The slide defines the desired shape of the photogenerated EHP. The rotation of the charge distribution is achieved by rotating the slide. A 1D scan of the carrier profile is taken at angles between 0° and 180°. For the experiment in Fig. 4 the picture of a double slit aperture was projected and rotated on the SAW path.

Fig. 4a shows scans for various angles. Using standard tomography backprojection techniques [10] we reconstructed the 2D charge distribution as shown in Fig. 4b and find the shape of the double slit aperture well reproduced. From the sharpness of the edges we get a spatial resolution of about 20 μm. Future work will be concentrated on the improvement of the spatial resolution and sensitivity. Moving to higher frequencies, i.e. shorter SAW wavelengths will improve both. Extremely high sensitivities can be achieved when hybrid materials are used and conventional semiconductor systems are combined with strong piezoelectric substrates.

To conclude, we demonstrated the imaging of carrier density profiles by surface acoustic waves with a resolution of a few acoustic wavelengths. Extremely narrow SAW paths were excited by tapered transducers and used to scan photogenerated charge distributions. The drag and transport of electrons and holes by

the coherent phonon wind of a high amplitude SAW could directly be observed at room temperature. The transition between the weak momentum transfer of the drag-effect and the complete trapping of carriers in the transport regime is detected at the fringe of a photogenerated electron–hole plasma. The sensitivity of the method allows for the comparison of room temperature dynamics with low-temperature experiments. By the use of a tomographic technique we were able to record and reconstruct 2D charge distributions.

Acknowledgements

We gratefully acknowledge the financial support by the Bayerische Forschungsstiftung BayFor (294d/98) and the Deutsche Forschungsgemeinschaft DFG. The work at UCSB has been supported through AFOSR (grant No F49620-94-1-0158) and the center for quantized electronic structures (QUEST).

References

[1] A. Wixforth, J.P. Kotthaus, G. Weimann, Phys. Rev. Lett. 56 (1986) 2104.
[2] A. Wixforth, J. Scriba, M. Wassermeier, J.P. Kotthaus, G. Weimann, W. Schlapp, Phys. Rev. B 40 (1989) 7874.
[3] R.L. Willet, R.R. Ruel, W. West, L.N. Pfeiffer, Phys. Rev. Lett. 71 (1993) 3846.
[4] W. Sauer et al., Appl. Phys. Lett., submitted for publication.
[5] L.M. Smith, J.S. Preston, J.P. Wolfe, D.R. Wake, J. Klem, T. Henderson, H. Morkoc, Phys. Rev. B 39 (1989) 1862.
[6] A.E. Bulatov, S.G. Tikhodeev, Phys. Rev. B 46 (1992) 15058.
[7] C. Rocke, S. Zimmermann, A. Wixforth, J.P. Kotthaus, G. Böhm, G. Weimann, Phys. Rev. Lett. 78 (1997) 4099.
[8] M. Rotter, A.V. Kalameitsev, A.O. Govorov, W. Ruile, A. Wixforth, Phys. Rev. Lett. 82 (1999) 2171.
[9] M. Streibl et al., Appl. Phys. Lett., submitted for publication.
[10] John C. Russ, The Image Processing Handbook, 2nd Ed., CRC, Boca Raton, FL, 1995, 674 pp.